I J M E M S, 5(2) July-December 2012, pp. 71-76

Evaluation of Local Thinning During Cup Drawing of Gas Cylinder Steel using Isotropic Criteria

A. CHENNAKESAVA REDDY*, M. VIDYA SAGAR AND G. SATISH BABU

Department of Mechanical Engineering, JNTUH. College of Engineering and Technology, Hyderabad
Andhra Pradesh, India, E-mail: dr_acreddy@yahoo.com

ABSTRACT

The cup drawing process is simulated with an implicit finite element analysis. The effect of local thinning on the cup drawing has been investigated. The thinning is observed on the vertical walls of the cup. The strain is maximum at the thinner sections.

Keywords: gas cylinder steel, implicit finite element analysis, local thinning, cup drawing

1. INTRODUCTION

There is a number of sheet metal forming methods that are frequently used. Bending, roll forming, stretch forming, shearing, drawing, rubber forming, spinning, super plastic forming, hydro forming are some common sheet metal forming methods. It is known that mechanical property changes occur on the sheet metal part while forming. These changes are effective on the strength of the part.

2. ISOTROPIC CRITERIA

Von Mises and Tresca (or maximum shear) criteria are the most common criteria among isotropic criteria:

$$\sigma_y = \sqrt{\frac{1}{2}\left[(\sigma_1-\sigma_2)^2+(\sigma_2-\sigma_3)^2+(\sigma_3-\sigma_1)^2\right]} \quad (1)$$

Physically, von Mises value is proportional to the distortion energy, which is stored in the elastically deformed material before yielding. Figure 1 is a representation of the von Mises criteria in principal stress space [1].

Tresca criterion is identical to von Mises for uniaxial loading but it is more conservative for any other stress state:

$$\sigma_y = \max\left[|\sigma_1-\sigma_3|,|\sigma_2-\sigma_3|,|\sigma_1-\sigma_2|\right] \quad (2)$$

Figure 2 shows both von Mises and Tresca criterion on π plane. π plane is obtained by viewing

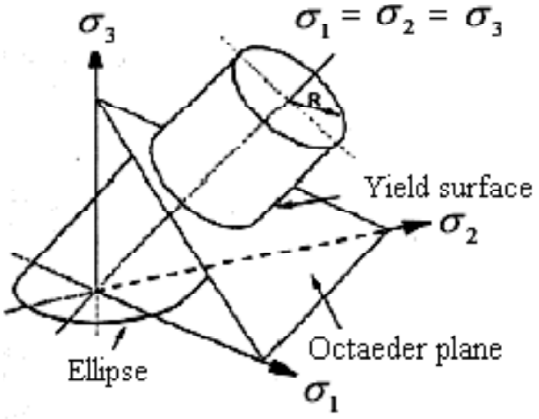

Figure 1: von Mises Surface in Principal Stress Plane

the principal stress plane through hydrostatic line (line on which $\sigma_1 = \sigma_2 = \sigma_3$) direction. As can be seen, Tresca criterion forms a hexagon into von Mises yield cylinder [2].

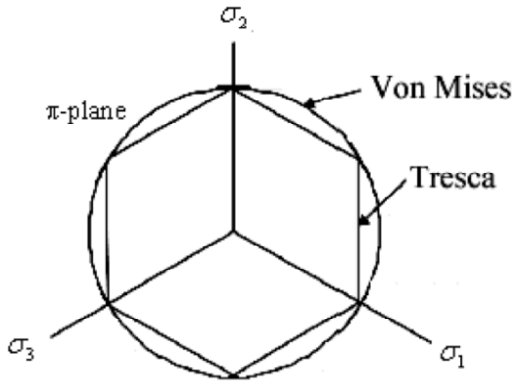

Figure 2: Tresca and von Mises Criteria on π-plane

Stress states inside the yield surface belong to elastic state of material. Stress states on the yield surface fit into plastic state. According to yield surface models there can not be any stress state outside of the yield surface. When some amount of load is applied to a material that is already at a stress state on the yield surface, yield surface changes. For hardening materials, produced stress state lies outside of the starting yield surface. During the load

Corresponding author: *dr_acreddy@yahoo.com

application, yield surface changes shape in such a way that, stress state always lies on the surface.

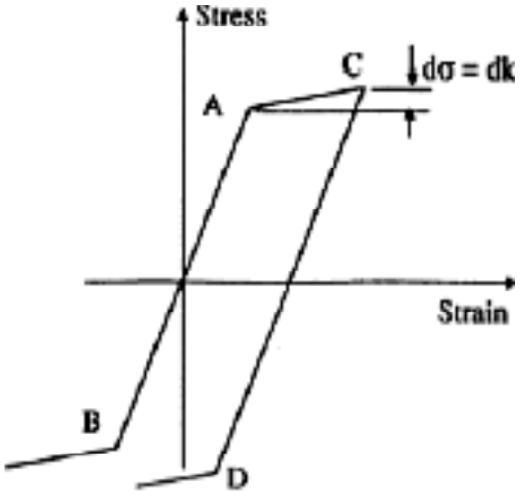

Figure 3: Loading / loading for Isotropic Hardening

The loading/unloading graph for isotropic hardening is demonstrated in figure 3. According to isotropic hardening, yield surface expands uniformly in stress plane as yielding occurs. Initially, the tensile and compressive yield stresses at points A and B are equal in magnitude. As the stress has exceeded the yield point in tension, the yield stress increases in both tension and compression. This is illustrated in figure 4 by the loading path from A to C, followed by unloading to zero stress and the compressive loading to the new compressive point D. The material remains isotropic after yielding and the new tensile and compressive stresses are equal in magnitude throughout the deformation history of the material.

Hill's model (Hill-1948) has advantages for the implementation finite elemt method (FEM) code. The model has the simple assumption of neglecting anisotropy. Additionally only three tensile tests at 0°, 45°, 90° are required to determine the material parameters.

The mathematical representation of Hill-48 model is as follows:

$$2f(\sigma_y) = F(\sigma_2-\sigma_3)^2 + G(\sigma_3-\sigma_1)^2 + H(\sigma_1-\sigma_2)^2 + 2L\tau_{23}^2 + 2M\tau_{31}^2 + 2N\tau_{12}^2 = 1 \quad (3)$$

where *F, G, H, L, M, N* are parameters characteristic of the current state of anisotropy. It is assumed that there is no Bauschinger effect and that hydrostatic stresses do not influence yielding. Therefore, linear terms are not included and Eq. 3 reduces to:

$$2f(\sigma_y) = F(\sigma_2-\sigma_3)^2 + G(\sigma_3-\sigma_1)^2 + H(\sigma_1-\sigma_2)^2 = 1 \quad (4)$$

Three tensile tests at 0°, 45°, and 90° directions are sufficient to determine three unknowns in Eq 42.6. Figure 5 shows these directions commonly used for sheet metals. MSC. Marc (FEM software) enables the user to enter the tensile test results, namely Lankford parameters, directly to utilize Hill-48 as yielding model.

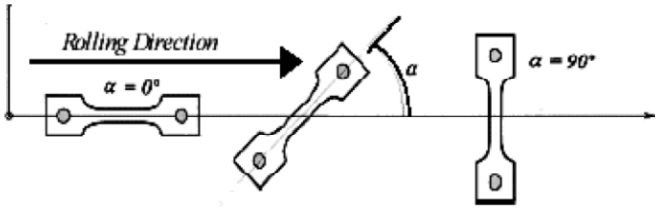

Figure 5: Tensile Test Directions for Hill Criteria Parameter Determination

Once the material stress-strain curve is obtained, several properties can also be calculated like modules of resilience etc. Ludwik's equation can be used to represent the plastic region of the monotonic true stress-true strain curve of metals as [3]:

$$\sigma_t = K\varepsilon_t^n \quad (5)$$

Or in logarithmic form:

$$\ln(\sigma_t) = \ln(k) + n\ln(\varepsilon_t) \quad (6)$$

where *K* and *n* are material constants, namely, the strength coefficient and the strain hardening exponent respectively. These constants are calculated from the stress-strain data obtained with tensile test.

Comparing least-squares method to Eq. (6)

$$y = A + Bx \quad (7)$$

where, $y = \ln(\sigma_t)$, $A = \ln(k)$, $B = n$ and $x = \ln(\varepsilon_t)$

The difference between a data point to the constructed line is:

$$\delta = y_i - (A + Bx_i) \quad (8)$$

The sum of squares of all errors:

$$E = \sum_{i=1}^{n} \delta_i^2 = \sum_{i=1}^{n} (y_i - A - Bx_i)^2 \quad (9)$$

To minimize the total error , the first derivatives are equated to zero;

$$\sum_{i=1}^{n} (y_i - A - Bx_i)(-1) = 0 \quad (10)$$

Simplifying,

$$\sum_{i=1}^{n} y_i = nA + B\sum_{i=1}^{n} x_i \tag{11}$$

Replacing parameters;

$$\sum_{i=1}^{n} x_i y_i = A\sum_{i=1}^{n} x_i + B\sum_{i=1}^{n} x_i^2 \tag{12}$$

The weighted average of n is calculated as follows:

$$\overline{n} = \frac{n_0 + 2n_{45} + n_{90}}{4} \tag{13}$$

The obtained value is represented with subscripts as $n_{x/y}$ where x is the angle to the rolling direction and y is the upper strain value of data points used for calculations. The mechanical properties of sheet metals exhibit anisotropy unless special operations to prevent directional property differences are done.

Lankford parameters are calculated at a certain strain level with the given formulation below:

$$r_{x/y} = \frac{\varepsilon_{t,w}}{\varepsilon_{t,t}} \tag{14}$$

where $\varepsilon_{t,w}$ is the true width strain and $\varepsilon_{t,t}$ is the true thickness strain. The subscript x is the angle to rolling direction and y is the strain level at which the calculation is made. The weighted average value of r is calculated as:

$$\overline{r} = \frac{r_0 + 2r_{45} + r_{90}}{4} \tag{15}$$

The objective of this paper is to study the effect of local thickness change on the sheet metal forming.

3. EXPERIMENTAL PROCEDURE

A double action hydraulic press with 2000 kN capacity is used for the drawing process of cup (figure 6). The chemical composition of material is given in Table 1. The material is gas cylinder steel with grade number P245NB.

Table 1
Chemical Composition of Gas Cylinder Steel, %wt

Material	*C*	*Si*	*Mn*	*P*	*S*	*Al*	*Ni*	*Ti*
Gas cylinder steel	0.15	0.10	0.40	0.015	0.01	0.02	0.009	0.03

Total process time is measured to be 8 seconds including edge trimming which is done before forming. Both sides of the blank are lubricated and the friction coefficient between blank and male pattern is assumed to be 0.12. Since thinner lubrication oil used for other faces, the friction coefficient between blank-female pattern, blank-blank holder is assumed to be 0.15.

The dimensions of the part drawn is given in figure 7, which is half of a pressure tube. The thickness of the sheet metal used is 2 mm. Blank is a 335 mm square before edge trimming. In the first action of the press, blank is trimmed into a 333 mm circular disk. Second action of the press forms the sheet into a half sphere-like shape as shown in figure 8. Thickness of the drawn cup is measured at several locations along the rolling and transverse directions.

Figure 6: Double Action Hydraulic Press

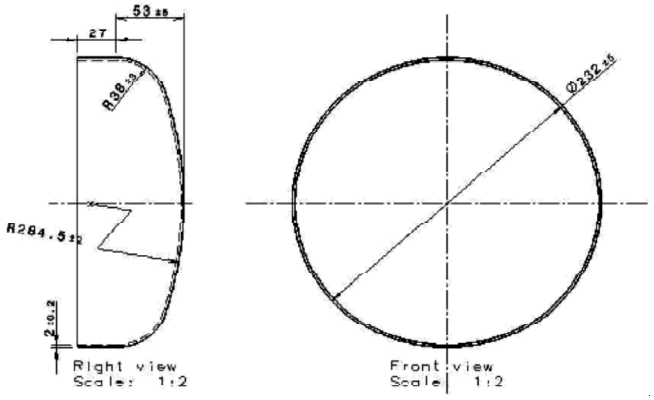

Figure 7: Dimensions of the Part Drawn

Figure 8: Drawn Cup

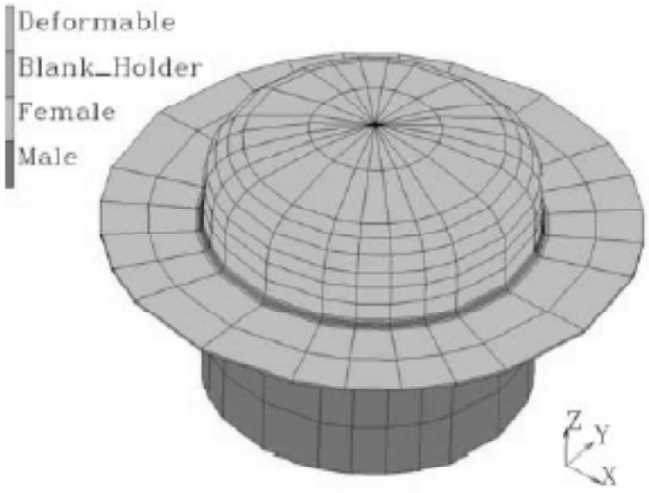

Figure 9: Parts of Rigid and Deformable Bodies in the Finite Element Model

4. FINITE ELEMENT MODELING

The geometric model was prepared in Catia V5r12. The finite element model of the process was organized in MSC Patran 2004r2 and MSC Marc 2003. In the drawing process of cup, there are three rigid and one deformable body in the finite element model. These bodies are shown in figure 9. The mesh of the deformable body was equipped considering the deformation of the forming process.

Reduced integration quad4 thick shell flat elements (Marc 140) with 7 layers and without mid-nodes were used. Total number of elements is 12,672. Since the results of simulation at each node and element must be directly transferred into another program, full model had to be utilized. Another reason of using a 3D model is that the use of anisotropic material properties is not available in symmetric FE models.

The FE model has three boundary conditions. One is the applied force to the female pattern. Blank holder applies half of the female load. The second boundary condition is also force boundary condition, using the same load as female pattern with a factor of 0.5. Third boundary condition is defined to prevent the free body motion of the blank in horizontal plane, especially before the parts get into contact. This is achieved by defining fixed displacements to the 1st and 2nd degrees of freedom of the center node of the blank body.

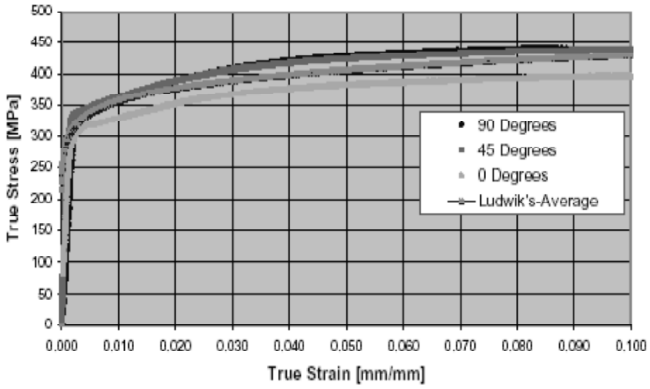

Figure 10: True Stress-true Strain Curve

Orthogonally anisotropic material properties were assumed and Hill-48 model was used. Elastic-plastic material plasticity was utilized with elastic-plastic stress-strain curve shown in figure 10. Von Mises yield criteria and isotropic hardening rule were employed.

The yield points of the material for different directions were found by offsetting the elastic curve of the true stress-true strain data by a value of 0.2%. Three tensile tests with samples taken in 0°, 45° and 90° directions to rolling direction of the sheet metal were carried out to find the parameters for the Hill-48 model. Lankford parameters for each direction were also calculated. The values obtained are tabulated in Table 2. The true stress-true strain curve was input into program with power method (Ludwik's function). The parameters K and n were calculated as described in Section 2. Ten data points are utilized for each direction of measurement and the average of three values is taken to find the values to be inputted into FE program. Subscript x in $n_{x/10}$ is the angle with respect to the rolling direction and 10 is the upper limit of true strain data in percentage used to calculate n.

Table 2
Calculated Values for K, N and Rat Different Angles to the Rolling Direction

	K	$n_{x/10}$	$r_{x/10}$
0^0	448	0.0502	2.037
45^0	538	0.0823	0.971
90^0	564	0.0938	0.137
Average	517	0.08	1.030

3D analysis is done with Marc2003 solver. Since displacements are large, large displacement option and large strain additive procedure for plasticity were used to invoke updated Lagrange procedure and to account for the effects of the internal stresses. The large displacement option automatically invokes the residual load correction procedure, which calculates the residual forces of the previous increment and corrects the loads of the next increment accordingly to enforce the global equilibrium that is very critical for load controlled problems where residual convergence checking is done. Coulomb friction model was employed for the friction modeling. Distance tolerance for the contact bias was set to 0.95 which gave better accuracy for contact detection. Relative sliding velocity was set to 1. Max cut-back number was increased to 30 because of stabilization problems. Relative residual force convergence was used for convergence checking with a value of 5%. 22 increments were set for totally 11 second analysis time. One load case was prepared for the formation of the sheet metal. Second one was set up for the release of contacts.

Analysis was restarted to reset relative sliding velocity, separation checking and penetration checking and convergence criteria for several times. Marc solver was able to restart from increment of recycle that was converged. Some of the parameters could be reset before restarting. Since the loads were very high at the advanced steps, 5% convergence in residual force was hard to obtain. At increment number 13, the convergence check was changed to 2.5% displacement. At increment number 17, convergence checking was set back to 5% residual force check with relative sliding velocity of 1.10^{-6}.

Another problem was high number of recycles because of touching, releasing or sliding nodes. These recycles in the analysis increment are called chattering. Chattering is more effective when bodies are getting into contact. At the beginning of the analysis, they were prevented by depressing the separation of nodes from a contact surface in an increment if the node came into contact with that surface in that increment. But at the advanced steps, this option was turned off to let the nodes separate from any contact body in any increment of the analysis.

5. RESULTS AND DISCUSSION

Thickness of the formed sheet was measured at several locations. The results from FE analysis and measurement are given in figure 11. Although there are some differences between analysis and measurements, general thickness distribution over the part is the similar. The maximum and minimum values and their locations were also calculated.

The thickness values from FE analysis are lower than the measure values as shown in figure 11. Maximum error occurs at the thinner region as 14%. There are not too much directional differences observed from the thickness change point of view as shown in figure 12. A very slight difference exists in the finite element analysis that part becomes 9% thinner at the rolling direction. This was expected since the material is normalized and material properties are close to each other as found by tensile tests. The thinning region is shown in figure 13. The thinning regions are observed on the vertical walls of the cup. The minimum thickness is 1.68 mm.

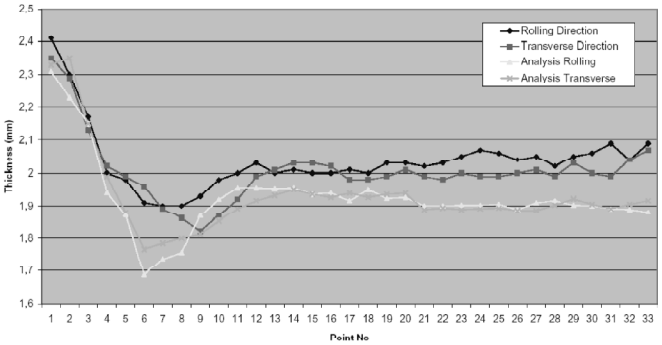

Figure 11: Thickness Values of Fe Analysis and Measurement

Figure 12: Thickness Distribution after Forming

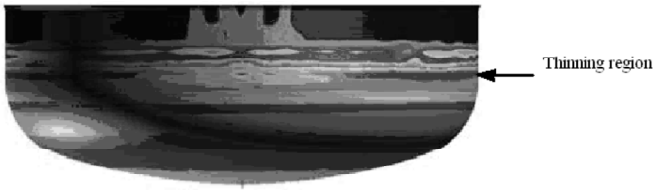

Figure 13: Illustration of Thinning Region

Figure 14: Total Equivalent Plastic Strain Distribution

Stress distribution over the part shows irregularities because of touching/releasing nodes on the deformable body. Figure 14 shows the total equivalence plastic strain. It is clear that the thickness changes directly effect the strain distribution over the region. The maximum strain occurs at thinner regions.

6. CONCLUSIONS

In this study, the effect of local thinning on the cup drawing is investigated with the help of finite element method and experimental procedure. The strain is maximum at the thinner sections. The thinning is observed on the vertical walls of the cup. The cup drawing process is simulated with an implicit algorithm. By this analysis, thickness changes are calculated.

References

[1] Shigley J. E. Mischke C. R., Standard Handbook of Machine Design, McGraw-Hill, Inc., New York, 1986.

[2] Stouffer C. D. Dame L. T., Inelastic Deformation of Metals, John Wiley & Sons, 2000.

[3] Fatigue Design Handbook, Society of Automotive Engineers, *3rd ed*., 1997.

[4] Vial C. Hosford W. F. Caddell R. M., Yield Loci of Anisotropic Sheet Metals; *Int. J. Mech. Sci*.; 1983, 25 -12.